Inorg. Chem. **2002**, *41*, 5495–5501

Expanding the Remarkable Structural Diversity of Uranyl Tellurites: Hydrothermal Preparation and Structures of $K[UO_2Te_2O_5(OH)]$, $Tl_3\{(UO_2)_2[Te_2O_5(OH)](Te_2O_6)\}\cdot 2H_2O$, β-$Tl_2[UO_2(TeO_3)_2]$, and $Sr_3[UO_2(TeO_3)_2](TeO_3)_2$

Philip M. Almond and Thomas E. Albrecht-Schmitt*

Department of Chemistry, Auburn University, Auburn, Alabama 36849

Received June 24, 2002

The reactions of $UO_2(C_2H_3O_2)_2\cdot 2H_2O$ with $K_2TeO_3\cdot H_2O$, Na_2TeO_3 and TlCl, or Na_2TeO_3 and $Sr(OH)_2\cdot 8H_2O$ under mild hydrothermal conditions yield $K[UO_2Te_2O_5(OH)]$ (**1**), $Tl_3\{(UO_2)_2[Te_2O_5(OH)](Te_2O_6)\}\cdot 2H_2O$ (**2**) and β-$Tl_2[UO_2(TeO_3)_2]$ (**3**), or $Sr_3[UO_2(TeO_3)_2](TeO_3)_2$ (**4**), respectively. The structure of **1** consists of tetragonal bipyramidal U(VI) centers that are bound by terminal oxo groups and tellurite anions. These UO_6 units span between one-dimensional chains of corner-sharing, square pyramidal TeO_4 polyhedra to create two-dimensional layers. Alternating corner-shared oxygen atoms in the tellurium oxide chains are protonated to create short/long bonding patterns. The one-dimensional chains of corner-sharing TeO_4 units found in **1** are also present in **2**. However, in **2** there are two distinct chains present, one where alternating corner-shared oxygen atoms are protonated, and one where the chains are unprotonated. The uranyl moieties in **2** are bound by five oxygen atoms from the tellurite chains to create seven-coordinate pentagonal bipyramidal U(VI). The structures of **3** and **4** both contain one-dimensional $^1_\infty[UO_2(TeO_3)_2]^{2-}$ chains constructed from tetragonal bipyramidal U(VI) centers that are bridged by tellurite anions. The chains differ between **3** and **4** in that all of the pyramidal tellurite anions in **3** have the same orientation, whereas the tellurite anions in **4** have opposite orientations on each side of the chain. In **4**, there are also additional isolated TeO_3^{2-} anions present. Crystallographic data: **1**, orthorhombic, space group *Cmcm*, $a = 7.9993(5)$ Å, $b = 8.7416(6)$ Å, $c = 11.4413(8)$ Å, $Z = 4$; **2**, orthorhombic, space group *Pbam*, $a = 10.0623(8)$ Å, $b = 23.024(2)$ Å, $c = 7.9389(6)$ Å, $Z = 4$; **3**, monoclinic, space group $P2_1/n$, $a = 5.4766(4)$ Å, $b = 8.2348(6)$ Å, $c = 20.849(3)$ Å, $\beta = 92.329(1)°$, $Z = 4$; **4**, monoclinic, space group $C2/c$, $a = 20.546(1)$ Å, $b = 5.6571(3)$ Å, $c = 13.0979(8)$ Å, $\beta = 94.416(1)°$, $Z = 4$.

Introduction

The uranyl tellurite system is currently represented by three minerals, cliffordite, $UO_2(Te_3O_7)$,[1] moctezumite, $PbUO_2(TeO_3)_2$,[2] and schmitterite, $UO_2(TeO_3)$,[3] and the synthetic phase, $Pb_2UO_2(TeO_3)_3$.[4] The remarkable feature of this poorly represented group is that there are few similarities between these compounds. For instance, $PbUO_2(TeO_3)_2$,[2] $UO_2(TeO_3)$,[3] and $Pb_2UO_2(TeO_3)_3$[4] all contain linear uranyl, UO_2^{2+}, moieties ligated by five oxygen atoms to create UO_7 pentagonal bipyramids, whereas $UO_2(Te_3O_7)$[1] contains UO_8 hexagonal bipyramids. Likewise, the coordination environments around the Te(IV) centers in these compounds show substantial variation. $PbUO_2(TeO_3)_2$ and $Pb_2UO_2(TeO_3)_3$ both contain C_{3v} tellurite, TeO_3^{2-}, anions,[2,4] whereas $UO_2(TeO_3)$ contains one-dimensional chains of corner-sharing square pyramidal TeO_4 units,[3] and $UO_2(Te_3O_7)$ possesses TeO_5 square pyramids.[1]

The differences in the structural building units in these compounds have dramatic effects on their dimensionality. $PbUO_2(TeO_3)_2$ is one-dimensional,[2] $UO_2(TeO_3)$ is two-dimensional,[3] and $UO_2(Te_3O_7)$[1] and $Pb_2UO_2(TeO_3)_3$ both have three-dimensional network structures.[4] In fact, $UO_2(Te_3O_7)$ is the only open-framework uranyl-containing compound that possesses UO_8 groups.[5] While two-dimen-

* Author to whom correspondence should be addressed. E-mail: albreth@auburn.edu.

(1) Branstätter, F. *Tschermaks Mineral. Petrogr. Mitt.* **1981**, *29*, 1.
(2) Swihart, G. H.; Gupta, P. K. S.; Schlemper, E. O.; Back, M. E.; Gaines, R. V. *Am. Mineral.* **1993**, *78*, 835.
(3) Meunier, G.; Galy, J. *Acta Crystallogr.* **1973**, *B29*, 1251.
(4) Branstätter, F. *Z. Kristallogr.* **1981**, *155*, 193.

10.1021/ic025820m CCC: $22.00
Published on Web 09/18/2002

sional structures dominate hexavalent uranium chemistry, one- and three-dimensional structures are much less common.[5] The predisposition of U(VI) compounds for adopting layered structures is a direct consequence of uranyl-containing polyhedra only being able to condense perpendicular to the terminal, trans dioxo, $(O{\equiv}U{\equiv}O)^{2+}$, unit.[5,6] Therefore, it is clear that there are structural features present in the uranyl tellurite system that allow for the formation of atypical structure types with dimensionalities both higher and lower than expected.

The ubiquitous presence of a stereochemically active lone-pair of electrons on the Te(IV) centers certainly plays a substantial role in the crystalline architecture of this family of compounds. However, the general tendency is for oxoanions of halogens or chalcogens with nonbonding electrons to either not affect the overall dimensionality of uranyl compounds or to reduce it from two-dimensional to one-dimensional, as demonstrated by approximately two dozen uranyl iodates[7−11] and selenites.[12−19] It is notable that none of these compounds contain three-dimensional uranium oxide networks. In fact, the preparation of three-dimensional network structures typically requires cross-linking of uranium oxide layers by additional building units as observed in the open-framework uranyl silicates, $Na_2(UO_2)(Si_4O_{10})\cdot 2.1H_2O$[20] and $RbNa(UO_2)(Si_2O_6)\cdot H_2O$,[20] or the orthogonal orientation of uranyl polyhedra with respect to one another as found for the organically templated uranyl phosphate $[(C_2H_5)_2NH_2]_2[(UO_2)_5(PO_4)_4]$[21] and for $(NH_4)_3(H_2O)_2\{[(UO_2)_{10}O_{10}(OH)][(UO_4)(H_2O)_2]\}$.[22] The ability of Te(IV) to bind four or five oxo groups in its inner-sphere, as observed in the unusual ternary phases, $BaTe_3O_7$,[23] $BaTe_4O_9$,[23] and $TeSeO_4$,[24] and in $UO_2(TeO_3)$[3] and $UO_2(Te_3O_7)$,[1] does not offer a satisfying explanation for the surprising behavior of uranyl tellurites because both $Pb_2UO_2(TeO_3)_3$ and $Na_8[(UO_2)_6(TeO_3)_{10}]$[25] contain only TeO_3^{2-} units, and yet they still adopt open-framework architectures.[4]

In this present study, we seek to expand the highly limited knowledge of the uranyl tellurite system through the hydrothermal preparation, structures, and properties of four new uranyl tellurites: two-dimensional $K[UO_2Te_2O_5(OH)]$ (**1**) and $Tl_3\{(UO_2)_2[Te_2O_5(OH)](Te_2O_6)\}\cdot 2H_2O$ (**2**), and one-dimensional β-$Tl_2[UO_2(TeO_3)_2]$ (**3**) and $Sr_3[UO_2(TeO_3)_2](TeO_3)_2$ (**4**). We have recently communicated the structures, properties, and DFT calculations of $Na_8[(UO_2)_6(TeO_3)_{10}]$ and α-$Tl_2[UO_2(TeO_3)_2]$.[25] These studies further support the iconoclastic nature of uranyl tellurites.

Experimental Section

Syntheses. $UO_2(C_2H_3O_2)_2\cdot 2H_2O$ (98.0%, Alfa-Aesar), Na_2TeO_3 (99.5%, Strem), $K_2TeO_3\cdot H_2O$ (97.0%, Strem), $Sr(OH)_2\cdot 8H_2O$ (99.999%, Alfa Aesar), and TlCl (99.9%, Alfa Aesar) were used as received. Distilled and Millipore filtered water with a resistance of 18.2 MΩ was used in all reactions. Reactions were run in Parr 4749 23-mL autoclaves with PTFE liners. SEM/EDX analyses were performed using a JEOL 840/Link Isis instrument. Typical results are within 4% of actual ratios determined from single-crystal X-ray diffraction experiments. IR spectra were collected on a Nicolet 5PC FT-IR spectrometer from KBr pellets. *Warning: While the $UO_2(C_2H_3O_2)_2\cdot 2H_2O$ contains depleted U, standard precautions for handling radioactive materials should be followed. Old sources of depleted U should not be used, as the daughter elements of natural decay are highly radioactive and present serious health risks.*

$K[UO_2Te_2O_5(OH)]$ (1). $UO_2(C_2H_3O_2)_2\cdot 2H_2O$ (180 mg, 0.629 mmol) and $K_2TeO_3\cdot H_2O$ (320 mg, 1.177 mmol) were loaded in a 23-mL PTFE lined autoclave followed by the addition of 1.5 mL of water. The autoclave was sealed and placed in a preheated furnace for 4 d at 180 °C. The box furnace was cooled at 9 °C/h to 23 °C. The product consisted of a clear and colorless solution over yellow prisms of **1**. The mother liquor with a pH of 10.2 was decanted from the crystals, and the crystals were washed with methanol and allowed to dry. Yield, 232 mg (83% yield based on U). EDX analysis for $K[UO_2Te_2O_5(OH)]$ provided a K/U/Te ratio of 1:1:2. IR (KBr, cm^{-1}): 860 ($\nu_{3[uranyl]}$, s), 827 ($\nu_{1[uranyl]}$, s), 803 (ν_{TeO}, m, sh), 776 (ν_{TeO}, s), 669 (ν_{TeO}, s, br), 639 (ν_{TeO}, s, br), 471 (δ_{TeO}, m), 446 (δ_{TeO}, w), 406 (δ_{TeO}, m).[26−28]

$Tl_3\{(UO_2)_2[Te_2O_5(OH)](Te_2O_6)\}$ (2) and β-$Tl_2[UO_2(TeO_3)_2]$ (3). $UO_2(C_2H_3O_2)_2\cdot 2H_2O$ (180 mg, 0.629 mmol), Na_2TeO_3 (320 mg, 1.177 mmol), and TlCl (200 mg, 0.834 mmol) were loaded in a 23-mL PTFE lined autoclave. A 1.5 mL portion of water was then added to the solids. The autoclave was sealed and placed in a preheated furnace for 3 d at 210 °C. The box furnace was cooled at 9 °C/h to 23 °C. The product consisted of a clear and colorless solution over yellow plates of **2**, orange rods of **3**, and orange blocks of α-$Tl_2[UO_2(TeO_3)_2]$.[25] The mother liquor with a pH of 10.3 was decanted from the crystals. The crystals were washed with methanol and allowed to dry. Yields for **2**, **3**, and α-$Tl_2[UO_2(TeO_3)_2]$ were 241 mg (60% yield based on U), 44 mg (10%), and 75 mg (17%),

(5) Burns, P. C.; Miller, M. L.; Ewing, R. C. *Can. Mineral.* **1996**, *34*, 845.
(6) Burns, P. C.; Ewing, R. C.; Hawthorne, F. C. *Can. Mineral.* **1997**, *35*, 1551.
(7) Sykora, R. E.; Wells, D. M.; Albrecht-Schmitt, T. E. *Inorg. Chem.* **2002**, *41*, 2304.
(8) Bean, A. C.; Albrecht-Schmitt, T. E. *J. Solid State Chem.* **2001**, *161*, 416.
(9) Bean, A. C.; Campana, C. F.; Kwon, O.; Albrecht-Schmitt, T. E. *J. Am. Chem. Soc.* **2001**, *123*, 8806.
(10) Bean, A. C.; Ruf, M.; Albrecht-Schmitt, T. E. *Inorg. Chem.* **2001**, *40*, 3959.
(11) Bean, A. C.; Peper, S. M.; Albrecht-Schmitt, T. E. *Chem. Mater.* **2001**, *13*, 1266.
(12) Almond, P. M.; Albrecht-Schmitt, T. E. *Inorg. Chem.* **2002**, *41*, 1177.
(13) Almond, P. M.; Peper, S. M.; Bakker, E.; Albrecht-Schmitt, T. E. *J. Solid State Chem.*, in press.
(14) Loopstra, B. O.; Brandenburg, N. P. *Acta Crystallogr.* **1978**, *B34*, 1335.
(15) Mistryukov, V. E.; Michailov, Y. N. *Koord. Khim.* **1983**, *9*, 97.
(16) Ginderow, D.; Cesbron, F. *Acta Crystallogr.* **1983**, *C39*, 1605.
(17) Ginderow, D.; Cesbron, F. *Acta Crystallogr.* **1983**, *C39*, 824.
(18) Koshenlinna, M.; Mutikainen, I.; Leskelae, T.; Leskela, M. *Acta Chem. Scand.* **1997**, *51*, 264.
(19) Koshenlinna, M.; Valkonen, J. *Acta Crystallogr.* **1996**, *C52*, 1857.
(20) (a) Li, Y.; Burns, P. C. *J. Nucl. Mater.* **2001**, *299*, 219. (b) Wang, X.; Haung, J.; Liu, L.; Jacobson, A. J. *J. Mater. Chem.* **2002**, *12*, 406.
(21) Danis, J. A.; Runde, W. H. Scott, B.; Fettinger, J.; Eichhorn, B. *Chem. Commun.* **2001**, *22*, 2378.
(22) Li, Y.; Cahill, C. L.; Burns, P. C. *Chem. Mater.* **2001**, *13*, 4026.
(23) Johnston, M. G.; Harrison, W. T. A. *J. Am. Chem. Soc.* **2002**, *124*, 4576.
(24) Porter, Y.; Bhuvanesh, N. S. P.; Halasyamani, P. S. *Inorg. Chem.* **2001**, *40*, 1172.
(25) Almond, P. M.; McKee, M. L.; Albrecht-Schmitt, T. E. *Angew. Chem., Int. Ed.*, in press.
(26) (a) Pracht, G.; Lange, N.; Lutz, H. D. *Thermochim. Acta* **1997**, *293*, 13. (b) Pracht, G.; Nagel, R.; Suchanek, E.; Lange, N.; Lutz, H. D. *Z. Anorg. Allg. Chem.* **1998**, *624*, 1355. (c) Schellenschläger, V.; Pracht, G.; Lutz, H. D. *J. Raman Spectrosc.* **2001**, *32*, 373. (d) Peter, S.; Pracht, G.; Lange, N.; Lutz, H. D. *Z. Anorg. Allg. Chem.* **2000**, *626*, 208.
(27) Nakamoto, K. *Infrared and Raman Spectra of Inorganic and Coordination Compounds*, 5th ed.; Wiley-Interscience: New York, 1997.
(28) Barlett, J. R.; Cooney, R. P. *J. Mol. Struct.* **1989**, *193*, 295.

Table 1. Crystallographic Data for $K[UO_2Te_2O_5(OH)]$ (**1**), $Tl_3\{(UO_2)_2[Te_2O_5(OH)](Te_2O_6)\}\cdot 2H_2O$ (**2**), β-$Tl_2[UO_2(TeO_3)_2]$ (**3**), and $Sr_3[UO_2(TeO_3)_2](TeO_3)_2$ (**4**)

	K−(**1**)	Tl−(**2**)	Tl−(**3**)	Sr−(**4**)
fw	661.34	1891.60	1029.97	1235.29
space group	*Cmcm* (No. 63)	*Pbam* (No. 55)	$P2_1/n$ (No. 14)	$C2/c$ (No. 15)
a (Å)	7.9993(5)	10.0623(8)	5.4766(4)	20.546(1)
b (Å)	8.7416(6)	23.024(2)	8.2348(6)	5.6571(3)
c (Å)	11.4413(8)	7.9389(6)	20.849(2)	13.0979(8)
α (deg)	90	90	90	90
β (deg)	90	90	92.329(1)	94.416(1)
γ (deg)	90	90	90	90
V (Å^3)	800.05(9)	1839.2(3)	939.5(1)	1517.9(1)
Z	4	4	4	4
T (°C)	−80	−80	−80	−80
λ (Å)	0.71073	0.71073	0.71073	0.71073
ρ_{calcd} (g cm^{-3})	5.491	6.817	7.282	5.406
μ(Mo Kα) (cm^{-1})	279.63	500.48	575.12	287.23
$R(F)$ for $F_o^2 > 2\sigma(F_o^2)$[a]	0.0171	0.0444	0.0284	0.0283
$R_w(F_o^2)$[b]	0.0411	0.0937	0.0683	0.0646

[a] $R(F) = \sum||F_o| - |F_c||/\sum|F_o|$. [b] $R_w(F_o^2) = [\sum[w(F_o^2 - F_c^2)^2]/\sum wF_o^4]^{1/2}$.

respectively. EDX analyses for $Tl_3\{(UO_2)_2[Te_2O_5(OH)](Te_2O_6)\}\cdot 2H_2O$ and β-$Tl_2[UO_2(TeO_3)_2]$ provided Tl/U/Te ratios of 3:2:4 and 2:1:2, respectively. IR (KBr, cm^{-1}) **2**: 863 ($\nu_{3[uranyl]}$, m), 827 ($\nu_{1[uranyl]}$, m), 743 (ν_{TeO}, w), 722 (ν_{TeO}, w), 670 (ν_{TeO}, s, sh), 652 (ν_{TeO}, s, br), 543 (δ_{TeO}, w), 470 (δ_{TeO}, w). **3**: 843 ($\nu_{3[uranyl]}$, m, sh), 823 (ν_{TeO}, m), 807 (ν_{TeO}, m), 777 ($\nu_{1[uranyl]}$, m, sh), 769 (ν_{TeO}, m), 753 (ν_{TeO}, s), 746 (δ_{TeO}, m, sh), 714 (ν_{TeO}, m, sh), 693 (ν_{TeO}, s), 637 (ν_{TeO}, s, br), 609 (ν_{TeO}, m, sh).[26−28]

$Sr_3[UO_2(TeO_3)_2](TeO_3)_2$ (4). $UO_2(C_2H_3O_2)_2\cdot 2H_2O$ (90 mg, 0.315 mmol), Na_2TeO_3 (150 mg, 0.677 mmol), and $Sr(OH)_2\cdot 8H_2O$ (60 mg, 0.226 mmol) were loaded in a 23-mL PTFE lined autoclave, and 1.5 mL of water was then added. The autoclave was sealed and placed in a preheated furnace for 4 d at 180 °C. The furnace was cooled at 9 °C/h to 23 °C. The product consisted of a clear and colorless solution over transparent yellow prisms of **4** and $Na_8[(UO_2)_6(TeO_3)_{10}]$.[25] The mother liquor with a pH of 10.3 was decanted from the crystals. The crystals were washed with methanol and allowed to dry. Yield, 65 mg (28.9% yield based on U). EDX analysis for $Sr_3[(UO_2)(TeO_3)_2](TeO_3)_2$ provided a Sr/U/Te ratio of 3:1:4. IR (KBr, cm^{-1}): 847 ($\nu_{1[uranyl]}$, m), 789 (ν_{TeO}, m), 768 (ν_{TeO}, m), 729 (ν_{TeO}, m, sh), 700 (ν_{TeO}, s), 684 (ν_{TeO}, s), 624 (ν_{TeO}, s, br), 431 (δ_{TeO}, w).[26−28]

Crystallographic Studies. Crystals of **1**−**4** suitable for single-crystal X-ray diffraction experiments were selected using a stereomicroscope and mounted on thin glass fibers with epoxy. These mounted crystals were secured on goniometer heads, cooled to −80 °C with an Oxford Cryostat, and optically aligned on a Bruker SMART APEX CCD X-ray diffractometer using a digital camera. A rotation photo was taken for each crystal, and a preliminary unit cell was determined from 3 sets of 30 frames with 10 s exposure times using SMART. All intensity measurements were performed using graphite monochromated Mo Kα radiation from a sealed tube with a monocapillary collimator. For all compounds, the intensities of reflections of a sphere were collected by a combination of 3 sets of exposures. Each set had a different ϕ angle for the crystal, and each exposure covered a range of 0.3° in ω. A total of 1800 frames were collected with an exposure time per frame of 30 s for **1**−**4**.

For **1**−**4**, determination of integral intensities and global cell refinement were performed with the Bruker SAINT (v 6.02) software package using a narrow-frame integration algorithm. A faced-indexed analytical absorption correction was initially applied using XPREP.[29] Individual shells of unmerged data were corrected analytically and exported in the same format. These files were subsequently treated with a semiempirical absorption correction by SADABS[30] with a $\mu\cdot t$ parameter of 0.[12,31] The program suite SHELXTL (v 5.1) was used for space group determination (XPREP), direct methods structure solution (XS), and least-squares refinement (XL).[29] The final refinements included anisotropic displacement parameters for all atoms and a secondary extinction parameter. Some crystallographic details are listed in Table 1; selected bond lengths and angles are available in Tables 2−5. Additional details can be found in Supporting Information.

Table 2. Selected Bond Distances (Å) and Angles (deg) for $K[UO_2Te_2O_5(OH)]$ (**1**)

U(1)≡O(1) (×2)	1.816(4)	Te(1)−O(2) (×2)	1.859(3)
U(1)−O(2) (×4)	2.249(3)	Te(1)−O(3)	2.072(3)
		Te(1)−O(4)	2.282(2)
O−Te−O Bond Angles for $[Te_2O_5(OH)]$			
O(2)−Te(1)−O(2)′	97.3(2)	O(3)−Te(1)−O(4)	171.8(2)
O(2)−Te(1)−O(3)	88.2(1) (×2)		
O(2)−Te(1)−O(4)	86.4(1) (×2)		

Table 3. Selected Bond Distances (Å) and Angles (deg) for $Tl_3\{(UO_2)_2[Te_2O_5(OH)](Te_2O_6)\}\cdot 2H_2O$ (**2**)

U(1)−O(1) (×2)	2.399(9)	Te(1)−O(1)	1.884(9)
U(1)−O(2)	2.43(1)	Te(1)−O(2)	2.043(3)
U(1)−O(8) (×2)	2.30(1)	Te(1)−O(3)	1.868(9)
U(1)≡O(9)	1.80(1)	Te(1)−O(4)	2.065(3)
U(1)≡O(10)	1.77(2)	Te(2)−O(5)	1.87(1)
U(2)−O(3) (×2)	2.405(9)	Te(2)−O(6)	2.073(6)
U(2)−O(4)	2.39(1)	Te(2)−O(7)	2.214(5)
U(2)−O(5) (×2)	2.279(9)	Te(2)−O(8)	1.840(9)
U(2)≡O(11)	1.81(1)		
U(2)≡O(12)	1.81(1)		
O−Te−O Bond Angles			
O(1)−Te(1)−O(2)	80.7(5)	O(5)−Te(2)−O(6)	86.0(5)
O(1)−Te(1)−O(3)	104.7(4)	O(5)−Te(2)−O(7)	84.1(5)
O(1)−Te(1)−O(4)	86.4(5)	O(5)−Te(2)−O(8)	100.0(4)
O(2)−Te(1)−O(3)	89.4(5)	O(6)−Te(2)−O(7)	169.3(6)
O(2)−Te(1)−O(4)	160.1(5)	O(6)−Te(2)−O(8)	93.7(6)
O(3)−Te(1)−O(4)	79.3(4)	O(7)−Te(2)−O(8)	83.9(6)

(29) Sheldrick, G. M. *SHELXTL PC, Version 5.0, An Integrated System for Solving, Refining, and Displaying Crystal Structures from Diffraction Data*; Siemens Analytical X-ray Instruments, Inc.: Madison, WI, 1994.

(30) *SADABS*. Program for absorption correction using SMART CCD based on the method of Blessing: Blessing, R. H. *Acta Crystallogr.* **1995**, *A51*, 33.

(31) Huang, F. Q.; Ibers, J. A. *Inorg. Chem.* **2001**, *40*, 2602.

Table 4. Selected Bond Distances (Å) and Angles (deg) for β-$Tl_2[UO_2(TeO_3)_2]$ (**3**)

U(1)−O(1)	2.243(6)	Te(1)−O(1)	1.869(5)
U(1)−O(3)′	2.256(5)	Te(1)−O(2)	1.833(5)
U(1)−O(4)	2.219(5)	Te(1)−O(3)	1.896(6)
U(1)−O(6)′	2.196(6)	Te(2)−O(4)	1.883(6)
U(1)≡O(7)	1.824(6)	Te(2)−O(5)	1.855(6)
U(1)≡O(8)	1.826(5)	Te(2)−O(6)	1.899(6)
	O−Te−O Bond Angles		
O(1)−Te(1)−O(2)	100.9(3)	O(4)−Te(2)−O(5)	101.4(3)
O(1)−Te(1)−O(3)	99.1(3)	O(4)−Te(2)−O(6)	96.6(3)
O(2)−Te(1)−O(3)	98.8(3)	O(5)−Te(2)−O(6)	92.9(3)

Table 5. Selected Bond Distances (Å) and Angles (deg) for $Sr_3[UO_2(TeO_3)_2](TeO_3)_2$ (**4**)

U(1)−O(1) (×2)	2.259(3)	Te(1)−O(1)	1.894(3)
U(1)−O(2) (×2)	2.237(3)	Te(1)−O(2)	1.876(3)
U(1)≡O(7) (×2)	1.809(3)	Te(1)−O(3)	1.833(3)
		Te(2)−O(4)	1.858(3)
		Te(2)−O(5)	1.860(3)
		Te(2)−O(6)	1.872(3)
	O−Te−O Bond Angles		
O(1)−Te(1)−O(2)	99.4(1)	O(4)−Te(2)−O(5)	93.8(1)
O(1)−Te(1)−O(3)	97.2(1)	O(4)−Te(2)−O(6)	93.1(1)
O(2)−Te(1)−O(3)	96.4(1)	O(5)−Te(2)−O(6)	104.5(1)

Results and Discussion

Syntheses. Under basic, mild hydrothermal conditions, $UO_2(C_2H_3O_2)_2{\cdot}2H_2O$ reacts with $K_2TeO_3{\cdot}H_2O$ to yield $K[UO_2Te_2O_5(OH)]$ (**1**) in 83% yield in the form of yellow prisms. This reaction is quite general in nature, and the K^+ can be substituted with other alkali, pseudo-alkali, and alkaline-earth metals. For example, the reaction of $UO_2(C_2H_3O_2)_2{\cdot}2H_2O$ with Na_2TeO_3 produces $Na_8[(UO_2)_6(TeO_3)_{10}]$ in 76% yield.[25] Likewise, because of solubility differences, multiple cations can be present in these reactions, but the final products will only incorporate one type of cation. This statement is supported by the reaction of $UO_2(C_2H_3O_2)_2{\cdot}2H_2O$ with TlCl and Na_2TeO_3 which produces $Tl_3\{(UO_2)_2[Te_2O_5(OH)](Te_2O_6)\}{\cdot}2H_2O$ (**2**), α-$Tl_2[UO_2(TeO_3)_2]$,[25] and β-$Tl_2[UO_2(TeO_3)_2]$ (**3**). The preparation of $Sr_3[UO_2(TeO_3)_2](TeO_3)_2$ (**4**) is also accomplished by using mixed-cation reactions. This product is isolated from the reaction of $UO_2(C_2H_3O_2)_2{\cdot}2H_2O$ with Na_2TeO_3 and $Sr(OH)_2{\cdot}8H_2O$. The most important feature in the preparation of uranyl tellurites is for reactions to occur in high pH media. Under acidic conditions, the Te(IV) is reduced to elemental tellurium, which is only partially alleviated by adding hydrogen peroxide to the reaction mixtures.

Structures. $K[UO_2Te_2O_5(OH)]$ (1). The two-dimensional structure of **1** is most similar to $UO_2(TeO_3)$, which consists of chains of edge-sharing pentagonal bipyramidal UO_7 polyhedra that edge-share with TeO_4 square pyramids that in turn corner-share to form one-dimensional chains.[3] In **1**, these one-dimensional chains of corner-sharing TeO_4 square pyramids occur again; however, alternating bridging oxygen atoms are actually hydroxyl groups. This creates an alternating short/long Te−O−Te−O−Te bonding pattern. The Te−O bond distance to the hydroxyl oxygen atom is 2.282(2) Å, whereas the Te−O bond distance to the unprotonated oxygen atom is 2.072(3) Å. The remaining Te−O bond distances to the oxygen atoms involved in binding the uranyl moieties are both 1.859(3) Å. An additional feature of these chains is that the thermal ellipsoids of the Te(IV) and oxygen centers within the chain are slightly elongated along the direction of chain propagation, suggesting a small Peierls distortion. The bond valence sum for the tellurium center was determined to be 3.96.[32,33]

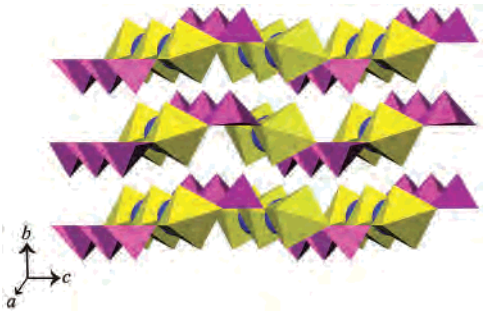

Figure 1. Depiction of the stacking of $K[UO_2Te_2O_5(OH)]$ layers in **1**.

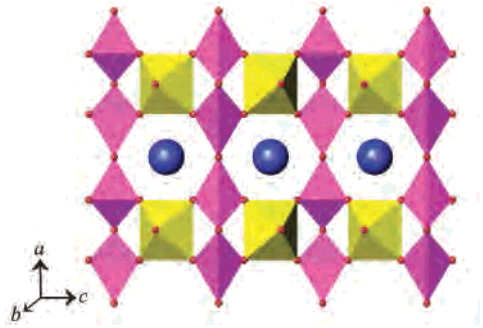

Figure 2. View down the *b*-axis showing the two-dimensional $^2_\infty[UO_2Te_2O_5(OH)]^{1-}$ sheets present in $K[UO_2Te_2O_5(OH)]$ (**1**). These sheets are composed of one-dimensional $^1_\infty[Te_2O_5(OH)]^{3-}$ chains that are bridged by uranyl moieties. In addition, there are crown-shaped cavities within the sheets that contain the K^+ cations.

The uranyl units in **1** are bound by oxygen atoms from the $^1_\infty[Te_2O_5(OH)]^{3-}$ chains to create tetragonal bipyramidal environments around the U(VI) centers. The uranyl moieties therefore serve to bridge the $^1_\infty[Te_2O_5(OH)]^{3-}$ chains to yield $^2_\infty[UO_2Te_2O_5(OH)]^{1-}$ sheets that extend in the [*ac*] plane as shown in Figure 1. Part of a $^2_\infty[UO_2Te_2O_5(OH)]^{1-}$ layer viewed down the *b*-axis is depicted in Figure 2. The U≡O bond distances within the uranyl unit are both 1.816(4) Å, while the remaining four U−O bond distances in the basal plane are 2.249(3) Å. Using these distances, the bond valence sum for the uranium center was calculated to be 6.10, which is in accord with U(VI).[6,32,33] An ORTEP diagram of the local environment of the U(VI) centers is illustrated in Figure 3.

The joining of the tellurium oxide chains by the uranyl units also creates voids within the sheets that are remarkably reminiscent of 18-crown-6. In fact, the K^+ cations in **1** reside within these cavities and form six $K^+{\cdots}O$ contacts, with four interactions of 2.807(3) Å and two of 2.925(1) Å. In addition, the K^+ cations form rather short ionic contacts of 2.716(4) Å with oxygen atoms from uranyl groups in adjacent layers.

(32) Brown, I. D.; Altermatt, D. *Acta Crystallogr.* **1985**, *B41*, 244.
(33) Brese, N. E.; O'Keeffe, M. *Acta Crystallogr.* **1991**, *B47*, 192.

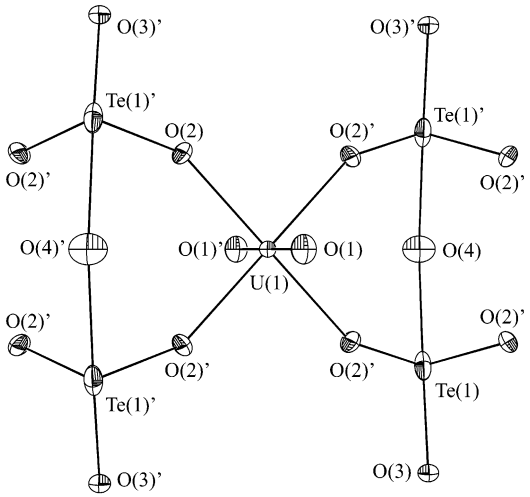

Figure 3. Illustration of the local environment of the uranium centers in $K[UO_2Te_2O_5(OH)]$ (**1**). 50% probability ellipsoids are shown.

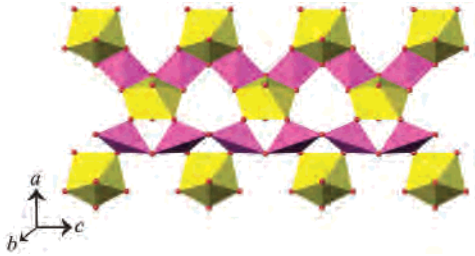

Figure 4. Depiction of part of a two-dimensional $^2_\infty\{(UO_2)_2[Te_2O_5(OH)](Te_2O_6)\}^{3-}$ sheet from $Tl_3\{(UO_2)_2[Te_2O_5(OH)](Te_2O_6)\}\cdot 2H_2O$ (**2**). The tellurium oxide chains take the form of corner-sharing TeO_4 square pyramids in one-dimensional $^1_\infty[Te_2O_6]^{4-}$ chains, and as partially protonated $^1_\infty[Te_2O_5(OH)]^{3-}$ chains similar to those found in $K[UO_2Te_2O_5(OH)]$ (**1**).

The eight coordinate environment for the K^+ cations observed here is quite similar to that of $[K(18\text{-crown-6})(DMF)_2]^+$.[34] In this latter cation, the $K^+\cdots O$ contact distances are as follows: 2.707(14) (×2) Å to the oxygen atoms of the dimethylformamide molecules, and 2.830(13) (×2), 2.775(14) (×2), and 2.707(14) (×2) Å to the oxygen atoms in the 18-crown-6 molecule. The average of the $K^+\cdots O$ contacts in **1** compares well with that of $[K(18\text{-crown-6})(DMF)_2]^+$ with distances of 2.81 and 2.77 Å, respectively. These data therefore support the role of the K^+ cations as structure-directing agents in the formation of **1**.

$Tl_3\{(UO_2)_2[Te_2O_5(OH)](Te_2O_6)\}\cdot 2H_2O$ (2). The structural features of **2** have similarities with both **1** and $UO_2(TeO_3)$.[3] First, there are two-dimensional $^2_\infty\{(UO_2)_2[Te_2O_5(OH)](Te_2O_6)\}^{3-}$ corrugated sheets formed from tellurium oxide chains and UO_7 pentagonal bipyramids as shown in Figure 4. The tellurium oxide chains take the form of corner-sharing TeO_4 square pyramids as found in $UO_2(TeO_3)$,[3] and as partially protonated $^1_\infty[Te_2O_5(OH)]^{3-}$ chains similar to those found in **1**. Furthermore, the sheets found in **2** are quite porous, and again, the countercations (Tl^+) are found within the layers instead of between them, as depicted in Figure 5. The water molecules are located between the layers and are not interacting with the U(VI) centers.

(34) Albrecht-Schmitt, T. E.; Ibers, J. A. *Inorg. Chem.* **1996**, *35*, 7273.

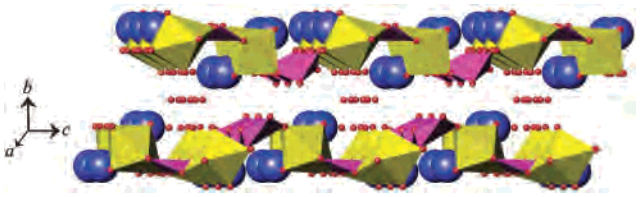

Figure 5. View of the packing of the corrugated $^2_\infty\{(UO_2)_2[Te_2O_5(OH)](Te_2O_6)\}^{3-}$ sheets in $Tl_3\{(UO_2)_2[Te_2O_5(OH)](Te_2O_6)\}\cdot 2H_2O$ (**2**). As found in **1**, the sheets are quite porous, and Tl^+ cations are found within the layers.

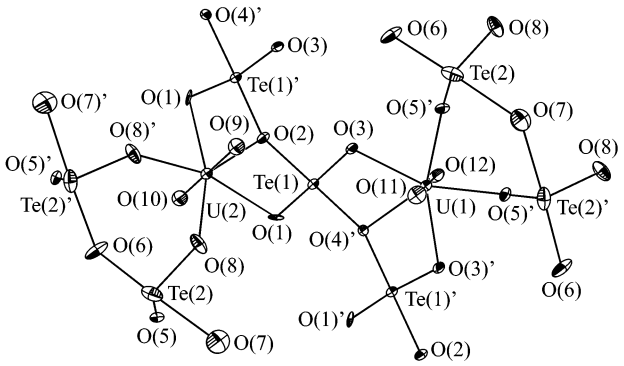

Figure 6. Illustration of the local environments of the uranium centers in $Tl_3\{(UO_2)_2[Te_2O_5(OH)](Te_2O_6)\}\cdot 2H_2O$ (**2**). 50% probability ellipsoids are shown.

There are two crystallographically unique U(VI) centers in **2**, both of which occur in uranyl moieties. Both uranyl groups form U—O bonds with both types of Te(IV) chains. An important structural difference between **1** and **2** is that alternating bridging oxygen atoms in the unprotonated chains in **2** are μ_3-O groups because they also bind the uranium atoms. This feature is absent in **1**, but present in $UO_2(TeO_3)$.[3] This means that each U(VI) center forms three U—O bonds with the one-dimensional $^1_\infty[Te_2O_6]^{4-}$ anionic chains and two U—O bonds with the $^1_\infty[Te_2O_5(OH)]^{3-}$ chains. The U≡O bond distances range from 1.77(2) to 1.81(1) Å, and the U—O bonds occur from 2.279(9) to 2.43(1) Å. An illustration of the local environments of the uranium centers in **2** is shown in Figure 6. The bond valence sum for the uranium centers in **2** were calculated at 6.01 and 5.93, which are both in agreement with U(VI).[6,32,33]

The Te—O bonds in the $^1_\infty[Te_2O_5(OH)]^{3-}$ chains show alternating short/long distances as found in **1**. Here, these distances are 2.073(6) and 2.214(5) Å. The shorter Te—O distances are with the oxygen atoms that are involved in bonding with the U(VI) centers. These distances are 1.840(9) and 1.87(1) Å. A small Peierls distortion evidenced by minor elongation of the Te(2) and O(7) thermal ellipsoids along the direction of chain propagation (*c*-axis) is also observed, as depicted in Figure 6. In contrast, the one-dimensional $^1_\infty[Te_2O_6]^{4-}$ chains show only small differences in the Te—O bonds involved in chain formation with distances of 2.043(3) and 2.065(3) Å. The remaining two Te—O bonds are 1.868(9) and 1.884(9) Å. The two unique Te(IV) centers in **2** have acceptable bond valence sums of 4.25 and 4.08.[32,33] There are three crystallographically unique Tl^+ cations in **2** that are present in environments with five to seven short $Tl^+\cdots O$ interactions, with contact distances ranging from 2.51(1) to 3.215(1) Å.

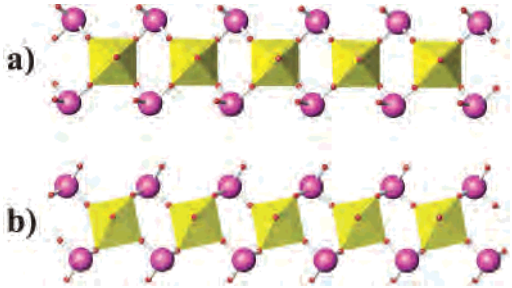

Figure 7. View of the one-dimensional $^1_\infty[UO_2(TeO_3)_2]^{2-}$ chains formed from uranyl units that are bridged by tellurite, TeO_3^{2-}, anions in β-$Tl_2[UO_2(TeO_3)_2]$ (**3**) (a) and $Sr_3[UO_2(TeO_3)_2](TeO_3)_2$ (**4**) (b). The chains differ between **3** and **4** in that all of the pyramidal tellurite anions in **3** have the same orientation, whereas the tellurite anions in **4** have opposite orientations on each side of the chain.

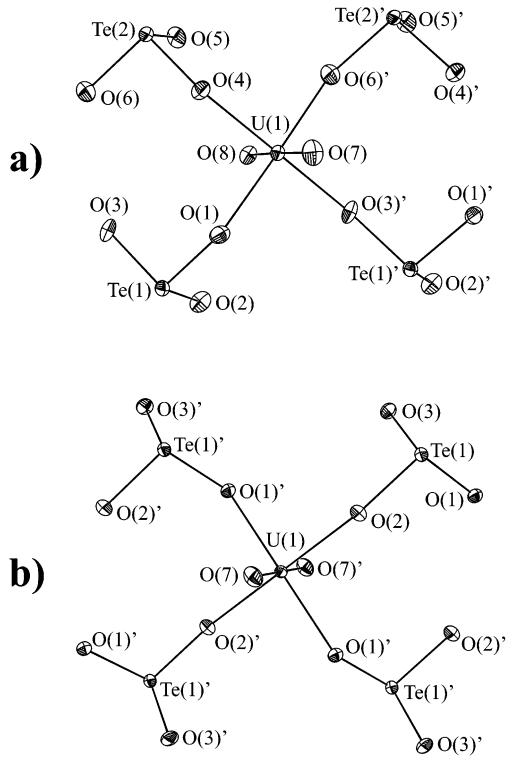

Figure 8. Tetragonal bipyramidal coordination environments for the U(VI) centers in β-$Tl_2[UO_2(TeO_3)_2]$ (**3**) (a) and $Sr_3[UO_2(TeO_3)_2](TeO_3)_2$ (**4**) (b). 50% probability ellipsoids are shown.

***β*-Tl$_2$[UO$_2$(TeO$_3$)$_2$] (3) and Sr$_3$[UO$_2$(TeO$_3$)$_2$](TeO$_3$)$_2$ (4).** The structures of **3** and **4** both contain one-dimensional $^1_\infty[UO_2(TeO_3)_2]^{2-}$ chains formed from uranyl units that are bridged by tellurite, TeO_3^{2-}, anions creating tetragonal bipyramidal environments around the U(VI) centers. These chains are shown in Figure 7. As demonstrated in this figure, the orientation of the tellurite anions is not the same between **3** and **4**. In **3**, all of the tellurite anions have their stereochemically active lone-pair of electrons oriented in the same direction making individual chains polar. In contrast, the tellurite anions in **4** have opposite orientation with respect to one another on each side of the chain. This latter topology has been recognized in the mineral derriksite, $Cu_4[(UO_2)(SeO_3)_2](OH)_6$,[35] where the tellurite anions are replaced by selenite anions. The local coordination environments for **3** and **4** are shown in Figure 8. In **3** and **4**, the Tl^+ or Sr^{2+} cations separate the chains from one another and balance charge. Unit cell packing diagrams for **3** and **4** are shown in Figures 9 and 10, respectively. An oddity of **4** is that there are additional isolated TeO_3^{2-} anions present between the chains.

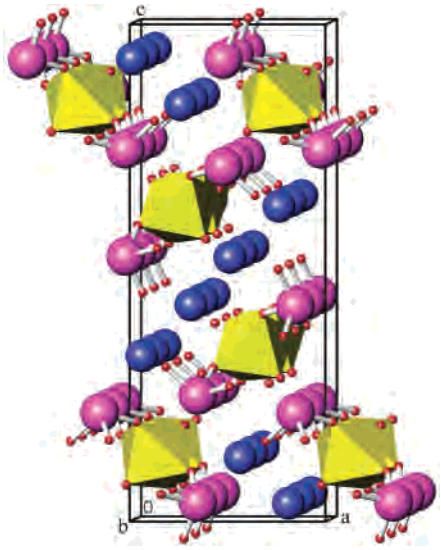

Figure 9. Packing of the one-dimensional $^1_\infty[UO_2(TeO_3)_2]^{2-}$ chains separated by Tl^+ cations in β-$Tl_2[UO_2(TeO_3)_2]$ (**3**) viewed approximately down the *b*-axis.

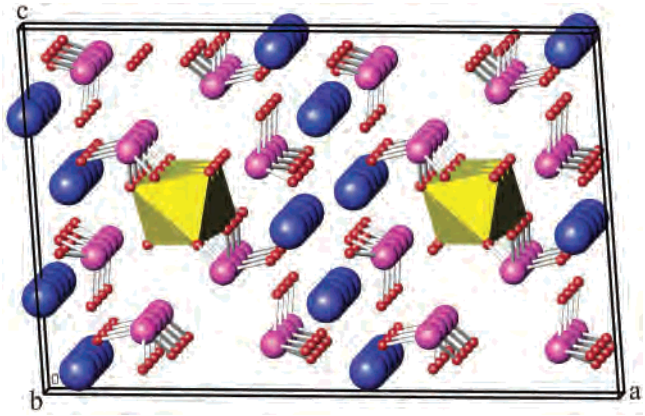

Figure 10. Depiction of the packing of the one-dimensional $^1_\infty[UO_2(TeO_3)_2]^{2-}$ chains, Sr^{2+} cations, and isolated TeO_3^{2-} anions in $Sr_3[UO_2(TeO_3)_2](TeO_3)_2$ (**4**).

There is only one type of U(VI) center in **3** and **4**, and the U≡O and U—O bond distances show only small variations with distances to the terminal oxo group ranging only from 1.824(6) to 1.809(3) Å, and U—O(TeO_3^{2-}) distances occurring from 2.196(6) to 2.256(5) Å for **3** and 2.237 to 2.259(3) Å for **4**. The bond valence sums for the uranium centers in **3** and **4** were calculated to be 6.16 and 6.15, which supports these compounds containing U(VI).[6,32,33] Likewise, the bond valence sums for the tellurium centers were found to be 4.06 and 4.04, both of which coincide with Te(IV).[32,33] The Te—O bond distances show variations based upon whether the oxygen atom is terminal or if it binds a uranium atom. The Te—O bond distances to the terminal oxo groups in the two independent tellurite anions in **3** have distances of 1.833(5)

(35) Ginderow, D.; Cesbron, F. *Acta Crystallogr.* **1983**, *C39*, 1605.

and 1.855(6) Å. In contrast, the Te—O bond distances with bridging oxygen atoms are universally longer and range from 1.869(5) to 1.896(6) Å. Similar features are also found for **4**. However, in **4** there is only one unique tellurite anion. Here, the Te—O distance to the terminal oxo group is 1.833(3) Å, while the bridging distances are 1.894(3) and 1.876(3) Å. The isolated tellurite anions have Te—O bond distances intermediate between the terminal and the bridging Te—O distances in the bound anion with an average Te—O distance of 1.863(3) Å.

Vibrational Spectroscopy. IR vibrational spectra for **1**−**4** were collected to determine the $[O{\equiv}U{\equiv}O]^{2+}$ symmetric ν_1 and asymmetric ν_3 vibrational frequencies, which are diagnostic of both the +6 oxidation state for uranium and the U≡O bond distance.[27,28] Some complications can arise in assigning these spectra because of overlap between the uranyl ν_1 mode and ν_1 modes from the tellurite anions. To aid in the assignment of the uranyl vibrational modes, the method of Bartlett and Cooney was used to calculate these frequencies.[28]

The uranium atom in **1** is located upon a 2/*m* site, precluding the observation of a ν_1 mode. The asymmetric ν_3 mode, however, is quite intense and was observed at 860 cm^{-1}. This vibrational mode was calculated at 858 cm^{-1}, which is in good agreement with the observed frequency. There are two crystallographically unique uranium centers in **2**, both of which are located on mirror sites. Here both the symmetric ν_1 and asymmetric ν_3 modes are observed at 827 and 863 cm^{-1}. If an average distance of 1.795 Å from the four U≡O bonds is used, then the calculated frequencies are determined to be 815 and 886 cm^{-1}, which differ significantly from the measured frequencies, and may be a consequence of having slightly different U≡O bond distances averaged together. The uranium atom in **3** is located on a general position, and as such both, the ν_3 and ν_1 modes were located at 843 and 777 cm^{-1}, with the latter assignment being only a guess because of the close proximity of tellurite modes. The calculated frequencies for **3** are 847 and 786 cm^{-1}. The U(VI) center in **4** is located on an inversion center eliminating the observation of a ν_1 mode in the IR spectrum as found in **1**. The ν_3 mode was observed at 847 cm^{-1} with a calculated frequency of 867 cm^{-1}. Again, poor agreement between the calculated and observed frequency is found. On the basis of these data, assignment of uranyl vibrational modes, particularly of the symmetric ν_1 mode, in the presence of oxoanions with heavy atom centers, such as iodate and tellurite, will be tenuous at best.

Conclusions

In this study, we have demonstrated that basic, mild hydrothermal conditions can be used to prepare novel uranyl tellurite phases. These compounds both duplicate structural features found in naturally occurring uranyl selenites and tellurites and provide access to new bonding motifs as in the one-dimensional $^1_\infty[Te_2O_5(OH)]^{3-}$ chains found in $K[UO_2Te_2O_5(OH)]$ (**1**) and $Tl_3\{(UO_2)_2[Te_2O_5(OH)](Te_2O_6)\}\cdot 2H_2O$ (**2**). We have also found the strongest evidence to date for the structure-directing effects of countercations in the preparation of purely inorganic uranyl phases. These compounds also help to further illustrate the trend toward dimensional reduction from two-dimensional layered structures that are most often observed for uranyl compounds to one-dimensional topologies when oxoanions with nonbonding electrons are incorporated.

Acknowledgment. This work was supported by the U.S. Department of Energy, Office of Basic Energy Sciences, Heavy Elements Program (Grant DE-FG02-01ER15187).

Supporting Information Available: X-ray crystallographic information for $K[UO_2Te_2O_5(OH)]$ (**1**), $Tl_3\{(UO_2)_2[Te_2O_5(OH)](Te_2O_6)\}\cdot 2H_2O$ (**2**), β-$Tl_2[UO_2(TeO_3)_2]$ (**3**), and $Sr_3[UO_2(TeO_3)_2](TeO_3)_2$ (**4**) in CIF format. This material is available free of charge via the Internet at http://pubs.acs.org.

IC025820M